Journal Pre-proof

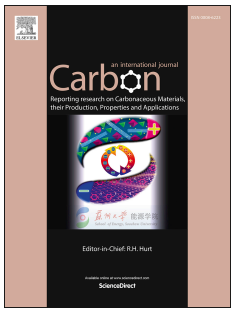

One-pot preparation of zwitterionic graphene nanosheets with exceptional redispersibility and its application in pickering emulsions

Jiawei Hu, Jiarui Hou, Shasha Huang, Lu Zong, Xiaodi Li, Zhijun Zhang, Yongxin Duan, Jianming Zhang

PII: S0008-6223(19)31081-4

DOI: https://doi.org/10.1016/j.carbon.2019.10.063

Reference: CARBON 14725

To appear in: *Carbon*

Received Date: 6 September 2019

Revised Date: 22 October 2019

Accepted Date: 23 October 2019

Please cite this article as: J. Hu, J. Hou, S. Huang, L. Zong, X. Li, Z. Zhang, Y. Duan, J. Zhang, One-pot preparation of zwitterionic graphene nanosheets with exceptional redispersibility and its application in pickering emulsions, *Carbon* (2019), doi: https://doi.org/10.1016/j.carbon.2019.10.063.

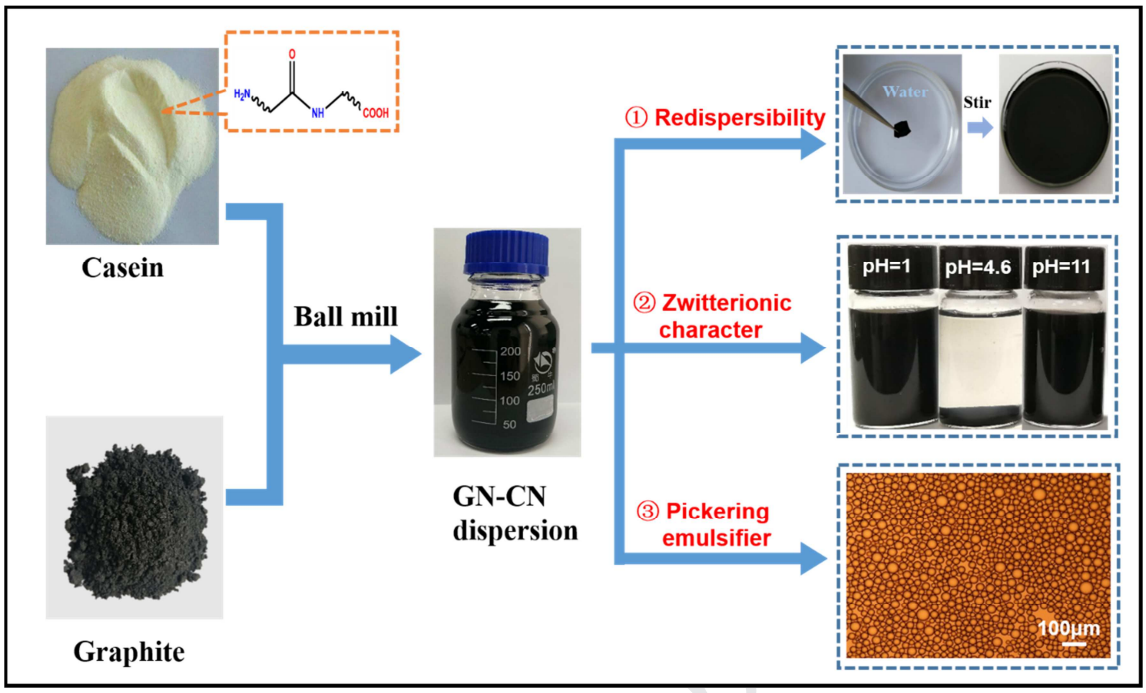

The facile preparation of zwitterionic graphene nanosheets with exceptional redispersibility and its a pplication as Pickering emulsifier have been demonstrated.

One-pot Preparation of Zwitterionic Graphene Nanosheets with Exceptional Redispersibility and Its Application in Pickering Emulsions

Jiawei Hu[a], Jiarui Hou[a], Shasha Huang[a], Lu Zong[a], Xiaodi Li[b], Zhijun Zhang[b], Yongxin Duan[a,] * and Jianming Zhang[a,] *

[a] Key Laboratory of Rubber-Plastics, Ministry of Education/Shandong Provincial Key, Qingdao University of Science & Technology, Qingdao City 266042, People's Republic of China.

[b] CAS Key Laboratory of Nano-Bio Interface, Suzhou Institute of Nano-Tech and Nano-Bionics, Chinese Academy of Sciences, Suzhou, Jiangsu, 215123, China.

*Corresponding author. Tel: +86-532-84022791. E-mail: zjm@qust.edu.cn (Jianming Zhang)

E-mail: dyx@qust.edu.cn (Yongxin Duan)

Abstract

Using biomass materials as exfoliating agents to produce graphene is a promising strategy due to their biocompatibility, reproducibility and sustainability. However, it's still a challenge to prepare high-concentration graphene dispersion using biomass exfoliating agents. Here, we present a green and facile method to prepare few layered graphene nanosheets in aqueous solution by one-pot ball milling in the presence of protein, casein (CN). The results show that CN protein could be acted as an efficient exfoliating and stabilizing agent, producing water-soluble graphene nanosheets with a concentration up to 2.14 mg ml^{-1}. As CN protein contains both amino and carboxyl groups, thus the prepared graphene nanosheets decorated with CN protein (GN-CN) show zwitterionically charged character and thereby can be stably dispersed under both acidic and alkaline conditions. Moreover, the oven-dried GN-CN hybrid exhibits exceptional redispersibility in water with a concentration as high as 100 mg ml^{-1} and even more. Benefiting from the zwitterionic character, GN-CN shows the Pickering emulsion effect over a wide pH range. As a proof of concept, the application of the zwitterionic GN-CN as a Pickering emulsifier to prepare microcapsule phase change composite material has been successfully demonstrated.

1. Introduction

As a result of the unparalleled physical properties and promising applications, graphene has attracted tremendous attention since its discovery in 2004[1, 2]. Although the unique two-dimensional (2D) structure gives it excellent mechanical strength (~1 TPa), superior electrical (6000 S cm^{-1}) and thermal conductivity (~5300 W m^{-1} K^{-1})[3-6], there are still many challenges to produce processable graphene nanosheets in large quantities and achieve suitable applications. Typically, liquid-phase

exfoliation by shear force or sonication is considered to more suitable for preparing high-quality and low-cost graphene on a large scale[7-10]. According to previous studies, suitable organic solvents[7, 11, 12] and some water dispersible stabilizers[1, 13-15] can serve as exfoliation media for exfoliating and stabilizing graphene nanosheets. Compared with organic solvents, stabilizer-assisted exfoliation in aqueous media is a green and promising way to produce highly dispersible graphene nanosheets. The adsorbed stabilizers on graphene surface prevent their stacking, making it a more stable dispersion. Moreover, noncovalent functionalization between stabilizers and graphene sheets endows graphene interesting properties, which can broaden the applications of graphene[15-18]. However, it should be pointed out that many stabilizers are synthesized by chemical method, which are toxic, environmentally unfriendly and non-renewable, and run counter to the theme of sustainable development[15, 18, 19].

Recently, some natural materials, such as gum arabic[17]and cellulose nanocrystal[20] have been used as intriguing liquid-phase exfoliating agents due to their biocompatibility, renewability and non-toxicity[16, 17, 20-25]. The resultant graphene nanosheets decorated with biomacromolecules via the covalent or non-covalent interaction exhibit remarkable stability, high yield and other interesting performance, attributed to synergetic effects between graphene and the corresponding biomacromolecules. As a typical biomacromolecule, protein exists widely in biology body of nature, such as plants, animals and microorganisms. A few studies demonstrated that some specific proteins are effective exfoliating agents for graphene and other two-dimensional materials in aqueous solutions[23-25]. As an example, Guan et al.[23] demonstrated bovine serum albumin can be used to exfoliate and stabilize graphene and other two-dimensional nanomaterials. In another work, Ge et al.[24] produced gelatin-adsorption graphene by sonication in gelatin solutions. The resultant graphene

significantly improves its compatibility with the gelatin substrate and the mechanical properties of their composites. However, the yield and concentration of graphene prepared with the two proteins are relatively low, so it is promising to explore a new protein to prepare high-concentration graphene dispersion with high efficiency.

Casein (CN) is a globular amphoteric protein with an isoelectric point (IP) of pH 4.6, and it is readily available from milk[26, 27]. Since the molecule contains both amino and carboxyl groups, CN can be dispersed in both acidic and alkaline conditions, which makes casein a zwitterionic protein. Meanwhile, CN exhibits many specific properties such as excellent emulsification, stability and adhesion due to its distinct amphiphilic structure. Therefore, we speculated that such a protein with both zwitterionic and amphiphilic structure might be used to exfoliate graphite into graphene nanosheets in the aqueous solution and endow the resultant graphene nanosheets zwitterionic character.

Herein, we presented the feasibility of CN-assisted exfoliation of graphene nanosheet by the one-pot ball milling method. Aqueous dispersions of few layered graphene nanosheets at high concentration have been successfully prepared. To one's surprise, the resultant GN-CN hybrid exhibits an extraordinary redispersibility in water with a high concentration (100 mg ml^{-1}). Moreover, the GN-CN is zwitterionic and shows doubly pH-responsive behavior due to the distinct chemical structure of CN protein. Finally, GN-CN was used to stabilize Pickering emulsion over a wide pH range and its application in the preparation of microcapsule phase change material was studied.

2. Experimental Section

2.1. Materials

Natural graphite (325 mesh, 99.95% purity) was purchased from Qingdao carbon Co. Ltd. CN

powder was purchased from Hua 'an Biological Products Co. LTD (Ningxia, China). Toluene was purchased from Chemical Industry Co. LTD (Shandong, China). CCK-8 (Cell Counting Kit-8) was purchased from Beyotime Biotechnology Co. Ltd (Shanghai, China). Calcien AM and propidium iodide (PI) were obtained from Solarbio life science Co. Ltd (Beijing, China). Stearic acid (SA) was obtained from Beilian Fine Chemicals Development Co. LTD (Tianjin, China).

2.2. Preparation of CN dispersion

CN dispersion was prepared by dissolving the CN powder in an alkaline solution. Typically, CN powder (10 g) was suspended in deionized water (85 g), and stirred at 400 rpm at 50 °C for 4 h. Then 25% ammonia (5 g) was added into the CN dispersion. After continuous stirring for 1 h to dissolve the CN, the solution was cooled down to room temperature to form a 10% CN aqueous dispersion. Prior to use, it was diluted to a designated concentrations using deionized water.

2.3. Preparation of graphene nanosheets decorated with CN (GN-CN)

Natural graphite powder (3 g) was first added in CN aqueous dispersions with different concentration (300 ml, 0.25 mg ml^{-1}-9 mg ml^{-1}). Then the mixtures were ball milled at 185 rpm for certain time (5-40 h) through a planetary ball mill machine (MITR-YXQM-2L) with the stainless steel grinding chamber having a volume of 0.5 L and four sizes of stainless steel mill balls (2 mm, 5 mm, 8 mm and 10 mm in diameter). Unexfoliated graphite was removed firstly by centrifugation at 4000 rpm for 30 min to remove the bulk graphite, and then was centrifuged at 8000 rpm for 30 min to remove the thick graphene sheets.

2.4. Preparation of wide pH-responsive Pickering emulsion

The Pickering emulsions were prepared by toluene (6 ml) and GN-CN dispersions (9 mg ml^{-1}, 3 ml) with different pH values. After mixing, the mixtures were emulsified with a homogenizer at 6000

rpm for 5 min at room temperature (RT). The pH of the GN-CN dispersions were adjusted by adding 0.5 M HCl or NaOH, and the resultant Pickering emulsions were observed and characterized after standing for 24 h at RT.

2.5. Cytotoxicity evaluation of GN-CN dispersion

CCK-8 assays were performed to evaluate the cytotoxicity of GN-CN dispersion. The procedure was as follows: MLg cells were incubated in DMEM-12 culture medium for 24 h and then incubated in GN-CN dispersions with different concentrations. After incubation for 24 h, the relative cell viability was checked by the CCK-8 assay. For live/dead cell staining, cell viability was tested by double-staining procedure using Calcien AM and propidium iodide (PI). In brief, after incubation for 24 h, cells were incubated with Calcien AM for 30 min at 37 °C. And then, cells were incubated with PI for 5 min at room temperature. After incubation, the samples were washed with phosphate buffer saline (PBS) twice and photographed using a Leica TCS SP5 confocal microscope. Cell viability was calculated via the staining images, in which the green and red fluorescence corresponded to the viable cells staining with Calcien AM and the dead cells staining with PI, respectively.

2.6. Preparation of composite microcapsule phase change materials (mPCMs)

The mPCMs was prepared by a Pickering emulsion method. Typically, SA (1 g) was added to a series of GN-CN dispersions (9 mg ml^{-1}, 10 ml) with different pH values, followed by heating the mixture to 90 °C in an oil bath to allow the melting of SA. Then, the mixture was emulsified with a homogenizer at 7000 rpm for 10 min to form an emulsion of SA microcapsule phase change materials, which was encapsulated by GN-CN. The resulting emulsions were allowed to cool naturally at RT for 24 h. To obtain the solid state mPCMs, the pH of emulsions were adjusted to near

the isoelectric point of CN to allow SA droplets encapsulated to settle. As-prepared solid mPCMs was dried at 50 °C for a night.

2.7. Characterization

UV-vis absorption were recorded using a UV–vis spectrophotometer (Shimadzu UV-2550) in the scanning range from 200 nm-800 nm. X-ray diffraction (XRD) of graphene nanosheets were characterized by an X-ray diffractometer (RIGAKU Ultima IV) using Cu Kα radiation (λ = 0.15406 nm). Raman measurements were performed with a Raman Spectrometer (InVia Series Laser Confocal Micro, RENISHAW) using a 532 nm excitation laser beam. Atomic force microscopy (AFM) images were taken using a Dimension Icon (BRUKER) with PeakForce Tapping mode. Transmission Electron microscopy (TEM) analyses were performed using a Tecnai F20 (FEI). Thermogravimetric analysis (TGA) was carried out using a Perkin Elmer TGA 6 (Perkin Elmer) with a heating rate of 10 °C/min ranging from 30 to 800 °C under nitrogen atmosphere. The Zeta Potential measurements were measured by a Dynamic Light Scattering (NanoBrook Omni) at 25 °C. The CD spectra were measured using a J-1500 CD Spectrometer (JASCO). The fluorescence images of cytotoxicity were photographed using a Leica TCS SP5 confocal microscope (Leica Microsystems, Germany). The optical micrographs of the prepared emulsions on transparent glass slides were taken using an ECLIPSE LV100N POL (Nikon). Differential scanning calorimetry (DSC) was tested using a Q20 (TA Instrument) at a heating and cooling rate of 20 °C/min. The morphology of phase change materials was observed using a Scanning Electron Microscope (JEOL SEM 6700).

3. Results and discussion

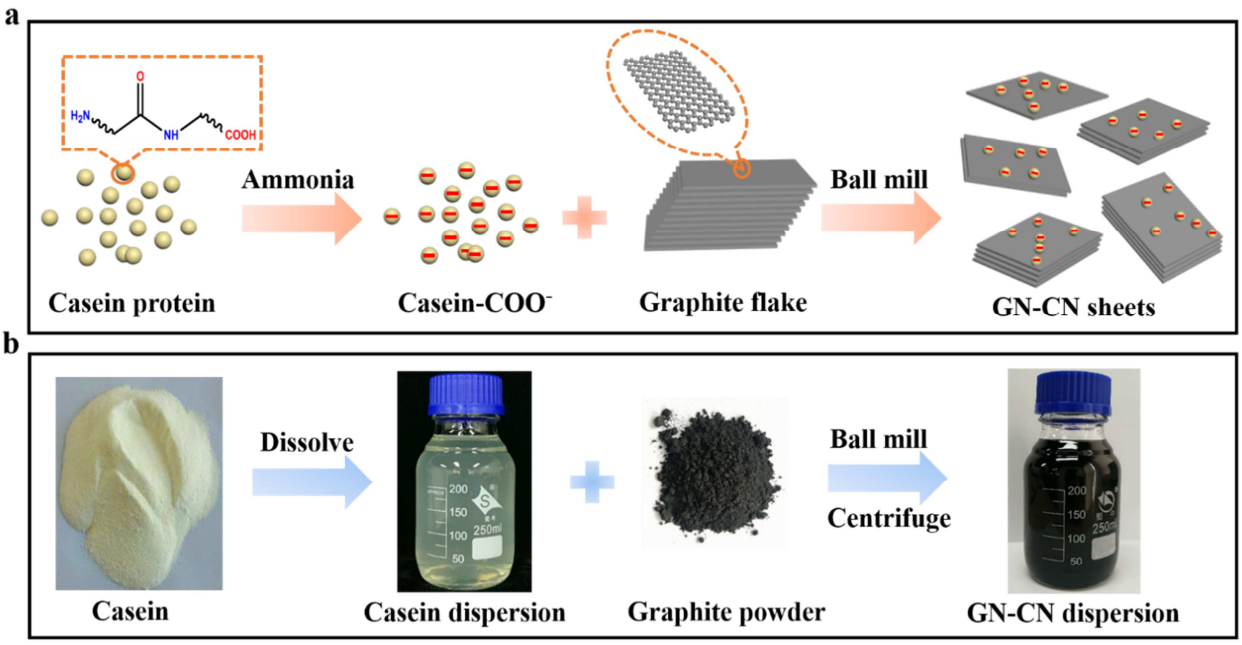

Figure 1. Schematic illustration of GN-CN preparation process. (a) Mechanism of exfoliation and stabilization of GN-CN sheets. (b) Ball milling exfoliation process of GN-CN in CN dispersion.

3.1. Preparation and Characterization of GN-CN dispersion

The preparation process is illustrated in Fig. 1. First, globular amphoteric CN was dissolved in deionized water by adding a certain mass of ammonia to obtain anionic charged CN dispersions (COO-) with high dispersion stability. Afterwards, the mixture of CN dispersion (COO-) and graphite was subjected to liquid-phase ball milling. Owing to the hydrophobic interaction between the CN molecular chains and the graphite sheets, the CN molecules were tightly adsorbed on the surface of the graphene sheets, resulting in the anionic charged graphene dispersion after ball milling. It's worth noting that as the pH value changes, the graphene sheets become positively charged due to the protonation of the amino group in the CN molecule, which will be confirmed in later.

Preparation conditions have a significant influence on the concentration of prepared graphene

dispersions and exfoliation efficiency according to previous study[20]. Here, we studied the effects of ball-milling time, CN concentration and pH of CN dispersion on graphene concentration and exfoliation efficiency. UV–vis spectroscopy was employed to evaluate the exfoliation efficiency. As shown in Fig. S1a, b, the absorption intensity at 264 nm increases with ball milling time within 40 h, indicating the increasing yield of graphene. However, longer ball milling time will damage the size and quality of the exfoliated graphene according to our previous research[16]. In addition, higher CN concentration will result in higher graphene yield within a certain concentration range of CN (Fig. S1c, d). The proportion of graphene in the prepared GN-CN was estimated from TGA profile (Fig. S2a). Fig. S2b shows that both graphene concentration and yield increase with the CN concentration but at the expense of decreasing graphene/GN-CN concentration ratio in the GN-CN dispersion. The highest graphene concentration and yield are 2.14 mg ml^{-1} and 21.4% respectively (Table S1), giving CN a distinct advantage over other natural materials which we will discuss in the following section. We predict that too high concentration of CN will reduce the concentration and yield of graphene due to the increasing viscosity and CN aggregation. Consider the effect of ball milling time and CN concentration comprehensively, the concentration of GN-CN dispersion used in our experiments and characterizations is both 1 mg ml^{-1} with 30 h ball-milling except for special instructions. In addition, the dependence of absorption intensity at 264 nm on pH of CN dispersion suggests that GN-CN dispersion can be prepared successfully only under strong acid and alkaline conditions in Fig. S3. That may be attributed to the better protonation of the amino and carboxyl groups facilitate the exfoliation and stabilization of GN-CN.

The UV–vis absorption spectrum for GN-CN dispersion was employed to study the conjugated structure of the exfoliated graphene nanosheets. As shown in Fig. 2a, compare with the negligible

absorption of CN, the UV–vis spectrum of GN-CN exhibits a strong absorption peak around 264 nm, which is ascribed to the π-π* transitions of aromatic C=C bonds[20]. The result demonstrates the conjugated structure of GN-CN nanosheets. The XRD pattern of the GN-CN nanosheets didn't show the reflection peaks at 26.5° from bulk graphite[28] in Fig. 2b, indicating that there is no stacking of layers, i.e., graphite was exfoliated into graphene nanosheets successfully. It's worth noting that the wide flat peak of GN-CN over a wide range (15-30°) may be attributed to the amorphous diffraction of CN. From the Raman spectrum of graphite in Fig. 2c, we observed that graphite exhibits its characteristic spectrum with a D band at 1348 cm^{-1}, G band at 1576 cm^{-1} and 2D band at 2706 cm^{-1} [20]. The strong D band and D' band at 1622 cm^{-1} in the Raman spectrum of GN-CN suggest the defects introduced during ball milling. Previous studies had proposed that the defects introduced in the process of mechanical exfoliation are mainly at the edges of graphene rather than the basal plane[9, 11, 25, 29, 30]. The layer number of graphene sheets was also estimated by analyzing Raman spectra. Compared with the graphite, the 2D band of GN-CN downshifts to lower frequency (15cm^{-1}), demonstrating the few layerd graphene nanosheets in the GN-CN dispersions[31]. Furthermore, related research proposed that the ratio of I_{2D}/I_G can be used to evaluate the number of graphene layers. It is calculated that the I_{2D}/I_G value is 0.59 for the GN-CN, corresponding to approximately 5 layers or less considering the aggregate of graphene sheets[32].

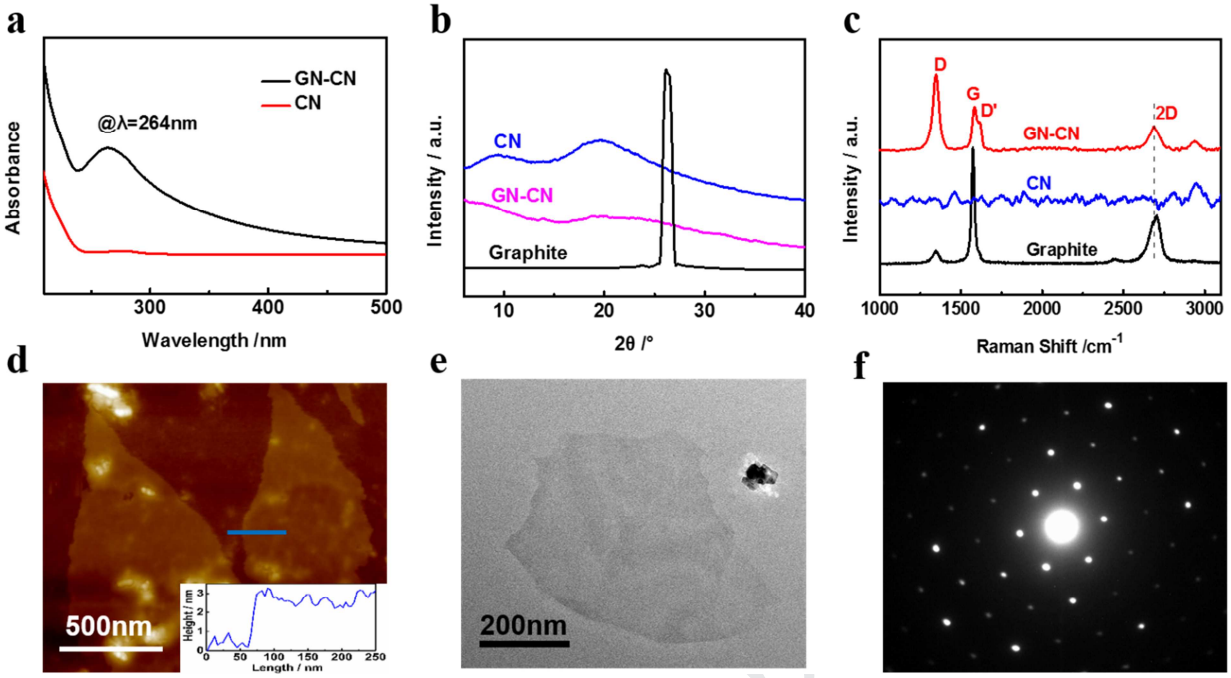

Figure 2. (a) UV–vis spectra of CN and GN-CN dispersion. (b) X-ray diffraction patterns of starting graphite, CN and GN-CN. (c) Raman spectra of GN-CN, CN and graphite. (d) AFM image of GN-CN with CN protein on its surface. (e) Typical TEM image of few layered GN-CN. (f) Selected-area electron diffraction (SAED) pattern of GN-CN.

The thickness and morphology of as-prepared GN-CN were further characterized by atomic force microscopy (AFM). Fig. 2d shows the thickness of a representative GN-CN from the as-prepared dispersion is about 2.05 nm, corresponding to 2–3 layer graphene sheets[1, 20, 24]. TEM image also provides evidence of few layered graphene exfoliation as shown in Fig. 2e. The selected area electron diffraction pattern (SAED) in Fig. 2f shows a typical hexagonal symmetry structure, confirming the high crystallinity of the GN-CN[33]. To find out more about the morphology of graphene and show statistical distributions of size and thickness of graphene, the GN-CN dispersion was further centrifuged at 12500 rpm for 30 min, and then the obtained sediment was re-dispersed in

deionized water of pH=10. Several other typical graphene nanosheets with lateral size in the range of tens of nanometers (Fig. S4) to tens of micrometers (Fig. S5) were also identified. The lateral size and thickness of 80 different graphene sheets were examined and the statistical distribution histograms were shown in Fig. S6. The large sized graphene sheets (lateral size larger than 2 μm) accounts for only 5% while the graphene sheets with lateral size within 400 nm accounts for 84%. Meanwhile, the thickness of graphene sheets is mainly distributed below 8 nm, accounting for 88%. These results indicate that the as-prepared GN-CN is mainly of small size and large sized graphene sheets are less abundant and can be negligible.

To characterize the stability of GN-CN dispersion, we measured the zeta potential of the GN-CN dispersions prepared with different ball milling time and CN dispersion concentration by dynamic light scattering. As shown in Fig. S7, almost all the GN-CN dispersions exhibit zeta potentials below -30 mV, indicating a certain amount of CN absorbed on the graphene nanosheets and formed a stable dispersion. The CD spectra of original CN dispersion and GN-CN dispersion were measured to determine whether the structure of CN was affected after ball milling. The CD spectra in Fig. S8 show that CN and GN-CN dispersions prepared with different CN concentration both exhibit negative absorption peaks at 201 nm, suggesting that the secondary structure of CN was not damaged and the CN remained stable. As a result, we conclude that CN is an efficient exfoliating and stabilizing agent for preparing few layered graphene nanosheets.

To compare CN with other nature materials used as exfoliating agents, the related information of graphene exfoliated were summarized in Table S2. Graphene concentration and yield are very important evaluation indicators for liquid-phase exfoliation of graphite. The results show that the concentration and yield of graphene using CN as exfoliating agent are higher than most of other

natural materials and all proteins (gelatin, HFBI and bovine serum albumin) listed in Table S2. In addition, we find it difficult to achieve the exfoliation of single layered graphene by using natural materials and the few, multilayers graphene and thick "graphite flake" are also a ubiquitous trend. Therefore, high concentration and yield GN-CN with different lateral size (from tens of nanometers to tens of micrometers) and thickness (few to multi layers) was successfully prepared.

The exfoliation mechanism of GN-CN can be explained by binding energy of CN on graphene layers. CN is an amphiphilic protein with distinct hydrophilic and hydrophobic regions, and will result in a binding energy due to the hydrophobic interaction between the hydrophobic part of CN and graphene layers. According to previous reports[23], the binding energies of different groups of protein on graphene vary greatly. The peptide bonds in the amino acid sequence of the protein will generate a strong binding energy on the graphene sheets, which will make the peptide bond tightly binding on the graphene surface, while the hydrophilic polar groups are exposed to the water. On the contrary, the nonpolar benzene rings in phenylalanine exhibit an unstable binding on the surface of graphene due to the weak binding energy. CN is a polymer consists of four types of CN monomers, α_{s1}-casein (α_{s1}-CN), α_{s2}-casein (α_{s2}-CN), β-casein (β-CN) and κ-casein (κ-CN) and each CN monomer has its own unique amino acids sequence[34]. The types and numbers of amino acids contained in the four CN are summarized in Table S3. We can calculate that the four CN contain a total of 784 amino acids, of which only 27 are phenylalanine. The resulting CN structure has a large proportion of peptide bonds but a slight amount of benzene rings provided by phenylalanine. Although the calculation is not accurate enough considering the different proportions of the four monomers in CN, we can qualitatively analyze the proportion of the benzene rings and the peptide bonds. Such a structure facilitates the tight binding of CN on the surface of graphene sheets and

forms graphene nanosheets decorated with CN during ball-milling, i.e. GN-CN.

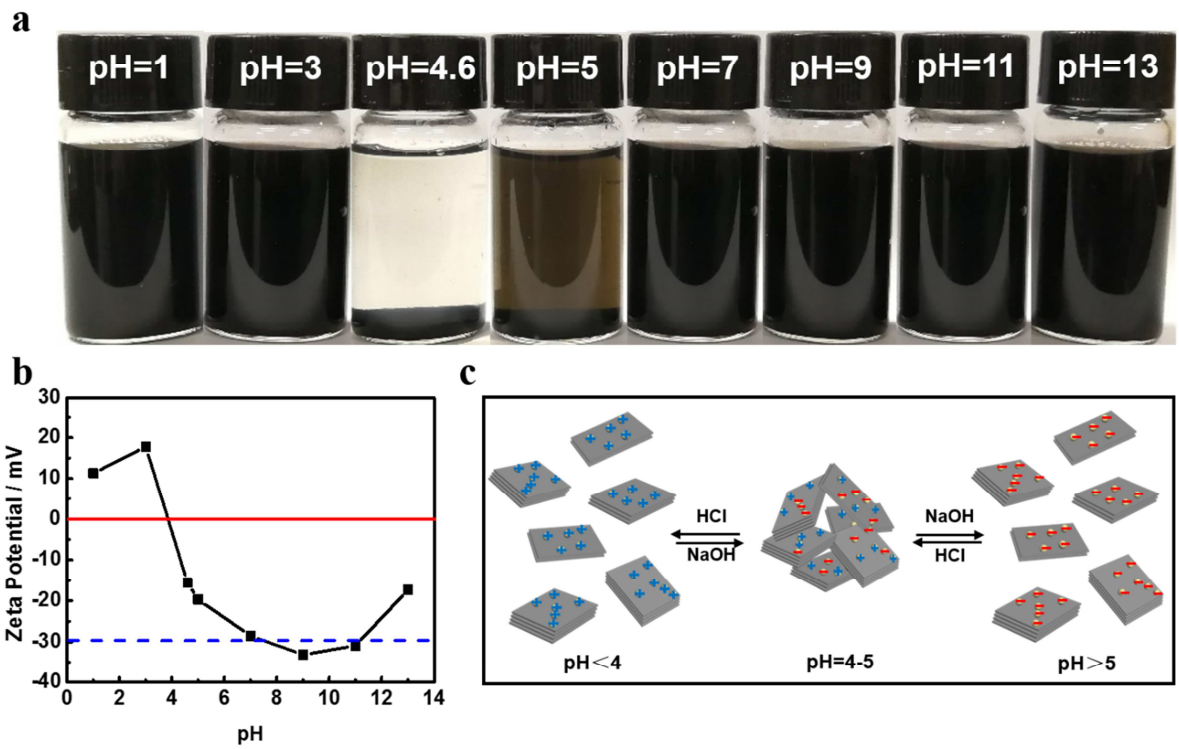

Figure 3. (a) Photographs of GN-CN dispersions with different pH from 1.0 to 13.0. (b) Zeta potential of GN-CN dispersions with a concentration of 1 mg ml^{-1} as a function of pH values. (c) Schematic illustration of GN-CN nanosheets' pH-responsive behavior.

3.2. Zwitterionic character of GN-CN

CN is an amphoteric protein with both amino and carboxyl groups on each end of the molecule chains. The special molecule structure endows it with an IP at around pH 4.6, at which the CN dispersion is unstable due to the absence of electrostatic repulsion. To determine whether the GN-CN exhibits the similar properties, we studied the stability of GN-CN dispersion at a series of pH values. Fig. 3a shows the stability of GN-CN dispersions at different pH values. It's obvious that GN-CN have aggregated at pH of near the IP of CN. To further understand the stability and surface charge of

GN-CN dispersion under different pH conditions, as shown in Fig. 3b, we studied the pH sensitivity of zeta potential of GN-CN. When the pH is above the IP of CN, carboxyl ionization on CN molecules makes GN-CN negatively charged, the electrostatic repulsion results in stable graphene dispersions. We find that the GN-CN dispersion exhibits higher stability at pH=7-11 with zeta potentials below -30 mV. Similarly, when the pH is below IP, graphene is positively charged due to amino protonation, and graphene will aggregate due to the weak electrostatic repulsion when the pH values is near the IP (pH=4-5). The change of zeta potential of GN-CN dispersion at acidic (pH=3) and alkaline (pH=9) condition was also examined over 15 days (Fig. S9). The small change of zeta potential and a negligible level of sediment in two months indicate that GN-CN can remain stable over two months. The above analyses indicate that we have prepared a stable zwitterionic graphene nanosheets with pH-responsive property.

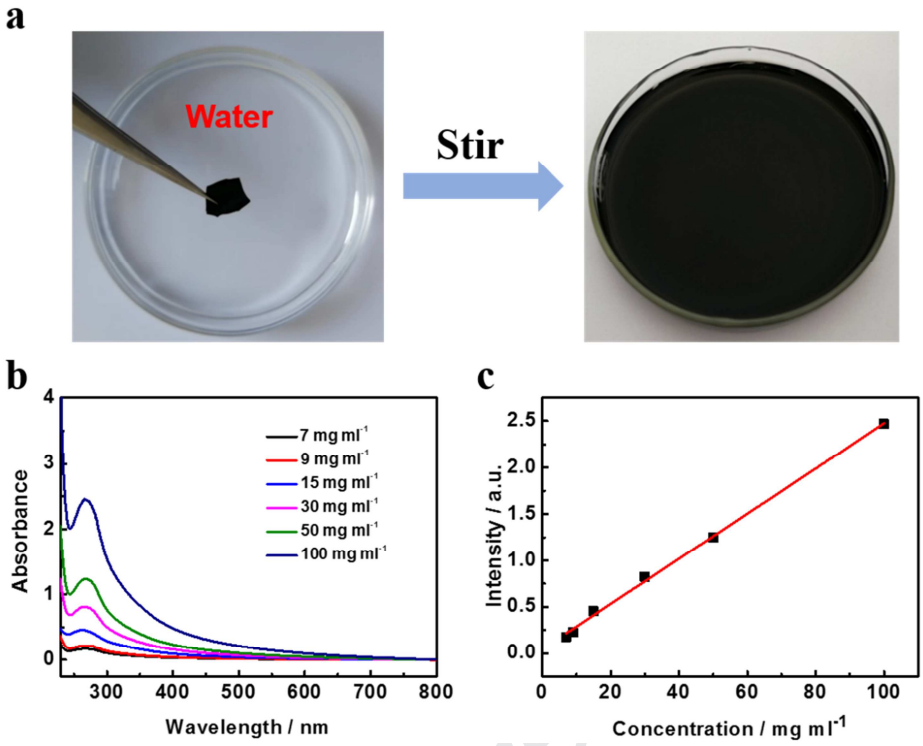

Figure 4. (a) Schematic illustration of the cast-drying GN-CN film was redispersed in water to form a homogeneous graphene dispersion. (b) UV-vis spectra of GN-CN in water at different concentrations of 7, 9, 15, 30, 50, 100 mg ml^{-1}, respectively. (c) The plot of the absorbance intensity versus the concentration.

3.3. Redispersibility of GN-CN

The redispersibility is of great significance for graphene, because solid state graphene is more favorable to practical application due to its convenient storage and easy transportation[35]. To evaluate the redispersibility of GN-CN, we dispersed the GN-CN film prepared by cast-drying into deionized water at room temperature. Interestingly, the GN-CN exhibits high re-dispersion concentration and fast dissolution rate simultaneously. As shown in Fig. 4a, a small piece of cast-drying GN-CN film was thrown into deionized water and stirred with a glass rod, then a homogeneous and stable GN-CN dispersion was formed. The redissolution process can be completed in a few minutes, which was

recorded by a video shown in Video. S1.

To ascertain the maximum concentration of GN-CN after re-dispersion, GN-CN dispersions with different concentrations were prepared by adding a certain amount of cast-drying GN-CN to 3 ml deionized water by sonication. To our surprise, the dispersion concentration of GN-CN was up to 100 mg ml^{-1} and corresponding concentration of graphene is 21.4 mg ml^{-1}. To the best of our knowledge, it's the highest dispersible concentration for liquid-exfoliated graphene. As shown in Fig. 4b, UV-vis spectra were measured for GN-CN dispersions with different concentration after redissolution. To ensure the transmittance of the high concentrated graphene, all specimens were diluted with deionized water to a factor of 100 before the test. The plot of the absorbance intensity at 264 nm as a function of GN-CN concentration was shown in Fig. 4c. The plot shows a good linear relationship when the GN-CN concentrations were below 100 mg ml^{-1}. We found that when the GN-CN concentration was above 100 mg ml^{-1}, the complete dissolution of GN-CN became difficult even with long sonication time. The re-dispersion property of GN-CN is attributed to the excellent solubility of CN in water at alkaline condition and its tight binding on graphene surface. When GN-CN was dispersed in water, CN dissolved and ionized rapidly and overcomes the π-π interaction between graphene sheets by electrostatic repulsion, resulting in a stable GN-CN dispersion. We tried to disperse the cast-drying GN-CN in different organic solvents by sonication but failed due to the insolubility of CN in organic solvents. The result demonstrates the important role of CN in the redispersibility of GN-CN.

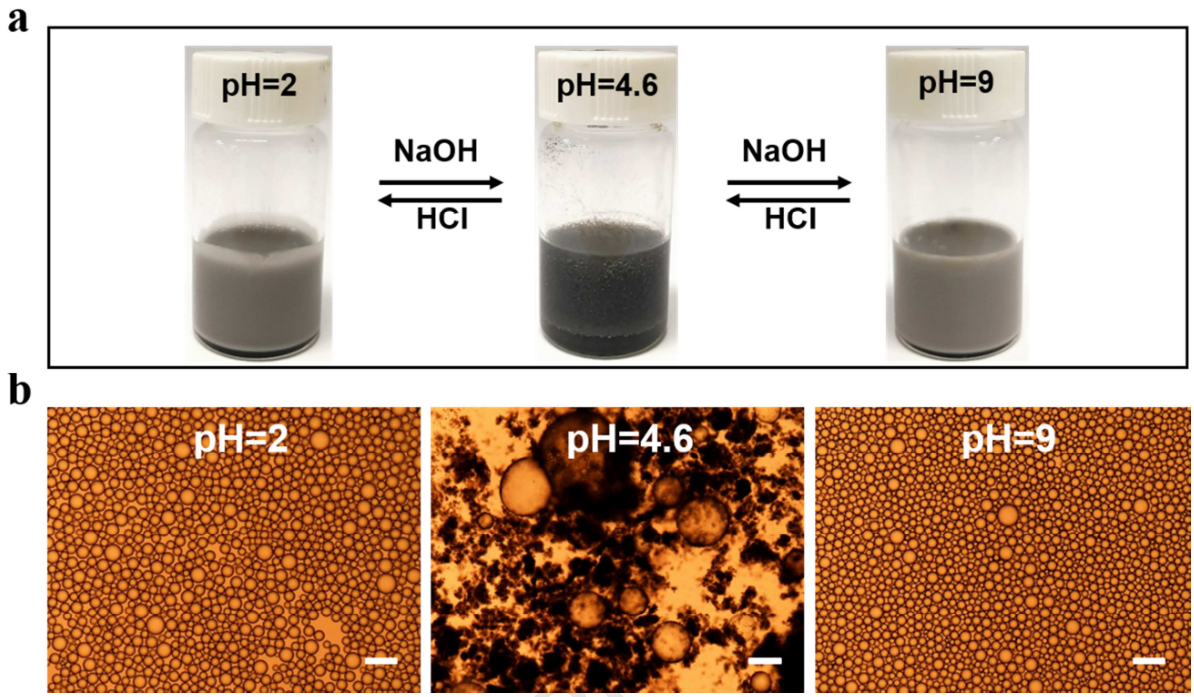

Figure 5. (a) Toluene-in-water emulsions prepared at different pH values using 9 mg ml^{-1} GN-CN dispersion. The volume ratio of toluene to water is 2:1. (b) Optical microscopy images of emulsions at the corresponding pH values. All scale bars are 100 μm.

3.4. Pickering emulsion stabilized by GN-CN

As we all know, Pickering emulsion is a solid colloidal emulsion stabilized by solid particles with moderate hydrophilicity and hydrophobicity. There are a few reports on the double electric emulsifier stabilizing Pickering emulsions[36, 37]. In order to study the potential of the zwitterionic GN-CN as Pickering emulsifier, the mixtures of toluene and GN-CN dispersions with different pH values were emulsified with a homogenizer. Toluene was used here because the π-π interaction between the benzene ring and graphene may facilitate producing stable emulsions with uniform size. Fig. 5a shows the effect of pH of GN-CN dispersions on emulsion stability. Stable emulsions are obtained

under both acidic (pH=2) and alkaline (pH=9) conditions and the spherical droplets are uniform in size with a diameter far less than 100 μm shown in Fig. 5b. However, the weak electrostatic interaction of GN-CN leads to strong hydrophobicity at pH near the IP of CN, which increases its affinity to oil phase. As a result, the GN-CN aggregates enter the toluene phase of the upper layer and few emulsion droplets with uniform size of several hundreds of micrometers were observed in Fig. 5b. The optical micrographs of emulsions over a wide pH range are shown in Fig. S10, indicating stable Pickering emulsions are obtained over a wide pH range except near the IP (pH 4-4.6). Furthermore, the size distributions of emulsion droplets were counted shown in Fig. S11. The result shows that more than 90% droplets of emulsions prepared at different pH values distribute between 10 and 50 μm in size. The emulsions prepared at pH=4 and 4.6 are not counted because it's hard to find enough droplets.

In order to explain the excellent emulsification effect of GN-CN, CN was used to emulsify toluene as a control under the same conditions with GN-CN. The optical microscopy images in Fig. S12 shows the similar emulsification effect of CN with GN-CN. We speculate the excellent emulsifying property may be attributed to the amphiphilic structure of CN and its tight binding to the graphene surface, which endows graphene a similar amphiphilic character. Such an amphiphilic GN-CN is very promising in emulsions field such as foods, cosmetics etc. Thus, it is necessary to evaluate biocompatibility of GN-CN by cytotoxicity test. The cytotoxicity was evaluated by culturing MLg cells with GN-CN dispersions for 24 h. The live/dead cell staining assay shows excellent cell viability and it's difficult to find significant dead cells (Fig. S13A). Furthermore, the CCK-8 assay result shows high cell viability varies in a narrow range of 93.6%-96.2% (Fig. S13B). The cell viability remained >93% even at a GN-CN concentration of 40 μg ml^{-1}, which is higher than that

culture with graphene oxide and other graphene exfoliated by exfoliating agents[38, 39]. The negligible cytotoxicity indicates that GN-CN has full potential for the above mentioned emulsion applications.

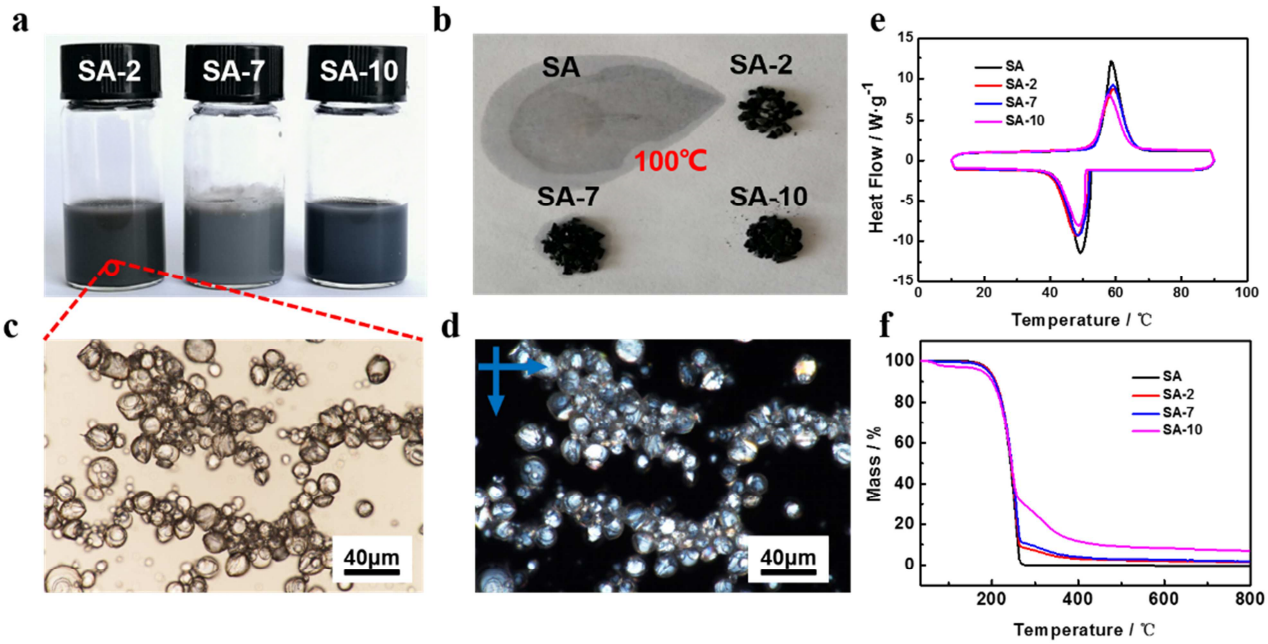

Figure 6. (a) Photographs of mPCMs emulsions emulsified at different pH values after cooling naturally at ambient temperature for 24h. (b) Photographs of SA and different mPCMs on a hot plate set 100℃. (c) Optical microscopy images of SA-2 emulsion. (d) Optical microscopy images of (c) after adding polarizer (e) DSC thermograms of SA and mPCMs. (f) TGA thermograms of SA and mPCMs.

3.5. Microcapsule phase change materials (mPCMs) prepared by GN-CN

Microcapsule phase change materials were considered promising thermal energy storage materials and possess high latent heat, high heat-transfer area and efficiency and exceptional shape stability due to unique core-shell structure[40, 41]. Graphene has been used as Pickering emulsifier to prepare mPCMs due to the excellent electronic, thermal properties and large surface area[40-43]. However, most

of graphene emulsifiers are obtained by physical decoration or chemical modification which may involve complex preparation process and toxic reagents. Considering facile preparation and environmental-friendly characteristics of GN-CN, we studied the potential of preparing mPCMs using GN-CN as Pickering emulsifier. To obtain mPCMs, the mixture of SA and GN-CN dispersion with different pH values was emulsified with a homogenizer at 90 °C.

Fig. 6a shows the appearance of mPCMs emulsion prepared with different GN-CN dispersions. For example. SA-2 is the mPCMs prepared with GN-CN dispersion of pH 2. It can be obviously observed the difference in colour of the three mPCMs emulsions. We put a drop of the SA-2 emulsion onto a slide and let it dry at room temperature for a while, then the morphology of SA-2 was observed by optical microscope shown in Fig. 6c. The SA capsules are spherical and the size is about 10-20 μm. Owing to the evaporation of water during the drying process, the SA capsules tend to come together. To illustrate the capsule is stearic acid microsphere, optical microscopy images of SA-2 after adding polarizer was observed as shown in Fig. 6d, the light sphere represents crystalline structure of stearic acid. Moreover, the microsphere is surrounded by a membrane-like structures, suggesting that SA was encapsulated by GN-CN and formed the core-shell structure. For comparison, the SA-7 and SA-10 exhibit irregular morphology shown in Fig. S14a, c. Interestingly, SA-10 exhibits a rod-like liquid crystal structure shown in Fig. S14d. The reason may be that sodium stearate was formed by the reaction of molten SA and sodium hydroxide under alkaline conditions at 90 °C, then the interaction between sodium stearate and GN-CN leads to the sodium stearate rod structure coated with GN-CN. The morphology of mPCMs was further confirmed by SEM shown in Fig. S15.

Table 1. Thermal properties of SA and mPCMs

	ΔH_m / J g^{-1}	T_m / □	ΔH_c / J g^{-1}	T_c / □
SA	196.2	58.63	194.5	49.27
SA-2	179.7	59.54	173.9	48.17
SA-7	174.5	59.15	167.8	48.54
SA-10	146.7	57.93	129.9	48.74

To investigate the thermal performance of mPCMs, the pH values of the emulsions were adjusted near the IP of CN. Then the sediments were collected by filtration and drying. Fig. 6b shows the photograph of SA and mPCMs on a hot plate at 100 °C. It's clear that SA has completely melted and the paper is soaked. SA-7 exhibits an obvious leakage, suggesting the melted SA can't be trapped effectively by GN-CN during the phase change process. The irregular core-shell structure of SA-7 also explains this phenomenon. However, SA-2 exhibits an excellent shape stability due to the effective trapping of melting SA cores, which prevents the melted SA from leakage. It was strange that SA-10 also didn't show significant leakage. That may have a lot to do with its liquid crystal structure and the formation mechanism of SA-10 need to be further explored and discussed. In addition, high latent heat is of great significance to mPCMs because it determines the energy storage potential. Therefore, DSC thermograms of mPCMs were measured as shown in Fig. 6e. The corresponding thermal properties data of SA and mPCMs were listed in Table 1. The heat of melting (ΔHm) and the heat of crystallization (ΔHc) of mPCMs are both lower than neat SA, indicating the existence of GN-CN component. Certainly, a decrease of GN-CN component will increase latent heat but at the expense of shape stability. SA-2, SA-7 and SA-10 exhibit ΔHm of 91.6%, 88.9% and 74.8% of neat SA respectively, indicating SA-2 possesses the highest latent. Meanwhile, the TGA

profile shows the highest weight loss occurs to SA-2, indicating the thinnest shell. It should be noted that the significant decrease of latent heat of SA-10 may be attributed to graphene's inhibition of SA crystallization due to the dispersion of graphene nanosheets in SA matrix[44]. We can conclude that an mPCMs with high latent heat and regular core-shell structure can be prepared at pH 2 using GN-CN as Pickering emulsifier.

4. Conclusions

In summary, we have demonstrated a green, facile and large-scale route to produce few layered graphene nanosheets decorated and stabilized by CN using a ball milling method. Benefiting from the strong hydrophobic interaction, CN can be used effective exfoliating and stabilizing agent. The resultant GN-CN shows exceptional redispersibility and dispersible concentration can be up to 100 mg ml^{-1} and even higher. Meanwhile, the aqueous GN-CN dispersion is stable under various pH values except near the IP of CN due to the weak electrostatic repulsion. Furthermore, the amphiphilic structure gives GN-CN excellent emulsifying property and it can be used as a good Pickering emulsion stabilizer over a wide pH values range, the negligible cytotoxicity makes GN-CN a potential candidate for emulsion applications in food and cosmetic fields. To explore the potential application of the GN-CN, SA/graphene composite microcapsule phase change material was successfully prepared at pH 2 using a Pickering emulsion technology, which GN-CN serves as an emulsion stabilizer. We presume that the novel graphene nanomaterial also can be used to prepare graphene/casein composite gel by cross-linking CN proteins through our preliminary attempt, or as an optical or electronic sensor.

Acknowledgements

The authors acknowledge the financial support from National Natural Science Foundation of China (51603112) and Taishan Mountain Scholar Foundation (TS20081120 and tshw20110510).

Appendix A. Supplementary data

Supplementary data associated with this article can be found, in the online version, at http://dx.doi.org/10.1016/j.carbon.

Reference

[1] M. Lotya, Y. Hernandez, P.J. King, R.J. Smith, V. Nicolosi, L.S. Karlsson, et al., Liquid phase production of graphene by exfoliation of graphite in surfactant/water solutions, J. Am. Chem. Soc. 131 (10) (2009) 3611-3620.

[2] A.K. Geim, K.S. Novoselov, The rise of graphene, Nat. Mater. 6 (2007) 183-191.

[3] T. Ma, Z.B. Liu, J.X. Wen, Y. Gao, X.B. Ren, H.J. Chen, et al., Tailoring the thermal and electrical transport properties of graphene films by grain size engineering, Nat. Commun. 8 (2017) 14486.

[4] A.C. Ferrari, F. Bonaccorso, V. Fal'ko, K.S. Novoselov, S. Roche, P. Boggild, et al., Science and technology roadmap for graphene, related two-dimensional crystals, and hybrid systems, Nanoscale. 7 (11) (2015) 4598-4810.

[5] E. Bourgeat-Lami, J. Faucheu, A. Noël, Latex routes to graphene-based nanocomposites, Polym. Chem. 6 (30) (2015) 5323-5357.

[6] Y. Zhu, S. Murali, W. Cai, X. Li, J.W. Suk, J.R. Pots, et al., Graphene and graphene oxide: synthesis, properties, and applications, Adv. Mater. 22 (2010) 3906-3924.

[7] Y. Hernandezl, V. Nicolosil, M. Lotyal, F. Blighel, Z.Y. Sun, S. De, et al., High-yield production of graphene by liquid-phase exfoliation of graphite, Nat. Nanotechnol. 3 (2008) 563–568.

[8] S. Sampath, A.N. Basuray, K.J. Hartlieb, T. Aytun, S.I. Stupp, J.F. Stoddart, Direct exfoliation of graphite to graphene in aqueous media with diazaperopyrenium dications, Adv. Mater. 25 (19) (2013) 2740-2745.

[9] L. Guardia, M.J. Fernandez-Merino, J.I. Paredes, P.Solís-Fernández, S.Villar-Rodil, A.Martínez-Alonso, et al., High-throughput production of pristine graphene in an aqueous dispersion assisted by non-ionic surfactants, Carbon 49 (5) (2011) 1653-1662

[10] Ciesielski. A, Samori. P, Graphene via sonication assisted liquid-phase exfoliation, Chem. Soc. Rev. 43 (1) (2014) 381-398.

[11] U. Khan, A. O'Neill, M. Lotya, S. De, J.N. Coleman, High-concentration solvent exfoliation of graphene, Small. 6 (7) (2010) 864-871.

[12] W.F. Zhao, M. Fang, F.R. Wu, H. Wu, L.W. Wang, G.H. Chen, Preparation of graphene by exfoliation of graphite using wet ball milling, J. Mater. Chem. 20 (2010) 5817-5819.

[13] R. Narayan, J. Lim, T. Jeon, D.J. Li, S.O. Kim, Perylene tetracarboxylate surfactant assisted

liquid phase exfoliation of graphite into graphene nanosheets with facile re-dispersibility in aqueous/organic polar solvents, Carbon. 119 (2017) 555-568.

[14] M. Lotya, P.J. King, U. Khan, S. De, J.N. Coleman, High-concentration, surfactant-stabilized graphene dispersions, ACS Nano. 4 (6) (2010) 3155-3162.

[15] Ciesielski. A, Samorì. P, Supramolecular approaches to graphene: from self-assembly to molecule-assisted liquid-phase exfoliation, Adv. Mater. 28 (29) (2016) 6030-6051.

[16] K. Wang, Q.Y. Ma, K. Pang, B.B. Ding, J.M. Zhang, Y.X. Duan, One-pot synthesis of graphene/chitin nanofibers hybrids and their remarkable reinforcement on poly(vinyl alcohol), Carbohydrate Polymers. 194 (2018) 146-153.

[17] J.C. Fan, Z.X. Shi, Y. Ge, J.L. Wang, Y. Wang, J. Yin, Gum arabic assisted exfoliation and fabrication of Ag–graphene-based hybrids, J. Mater. Chem. 22 (2012) 13764-13772.

[18] J. Cho, I. Jeon, S.Y. Kim, S. Lim, J.Y. Jho, Improving dispersion and barrier properties of polyketone/graphene nanoplatelet composites via noncovalent functionalization using aminopyrene, ACS Appl. Mater. Interfaces. 9 (33) (2017) 27984-27994.

[19] D.H. Duan, H.J. Ye, N. Meng, C.F. Xu, B. Han, Y.F. Chen, et al., Efficient exfoliation of graphite in chloroform with a pyrene-containing hyperbranched polyethylene as stabilizer to render pyrene-functionalized high-quality graphene, Carbon. 136 (2018) 417-429.

[20] P.M. Carrasco, S. Montes, I. Garcı´a, M. Borghei, H. Jiang, I. Odriozola, et al., High-concentration aqueous dispersions of graphene produced by exfoliation of graphite using cellulose nanocrystals, Carbon. 70 (2014) 157-163.

[21] A. Hajian, S.B. Lindström, T. Pettersson, M.M. Hamedi, L. Wagberg, Understanding the dispersive action of nanocellulose for carbon nanomaterials. Nano Lett. 17 (2017) 1439-1447.

[22] V. Chabot, B. Kim, B. Sloper, C. Tzoganakis, A.P. Yu, High yield production and purification of few layer graphene by Gum Arabic assisted physical sonication, Sci. Rep. 3 (2013) 1378.

[23] G.J. Guan, S.Y. Zhang, S.H. Liu, Y.Q. Cai, M. Low, C.P. Teng, et al., Protein induces layer-by-layer exfoliation of transition metal dichalcogenides, J. Am. Chem. Soc. 137 (2015) 6152-6155.

[24] Y. Ge, J.L. Wang, Z.X. Shi, J. Yin, Gelatin-assisted fabrication of water-dispersible graphene and its inorganic analogues, J. Mater. Chem. 22 (2012) 17619-17624.

[25] P. Laaksonen, M. Kainlauri, T. Laaksonen, A. Shchepetov, H. Jiang, J. Ahopelto, et al., Interfacial engineering by proteins: exfoliation and functionalization of graphene by hydrophobins, Angew. Chem. Int. Ed. 49 (2010) 4946-4949.

[26] C. Holt, Structure and stability of bovine CN micelles, Advances in Protein Chemistry. 43 (1992) 63-151.

[27] Y.D. Livney, Milk proteins as vehicles for bioactives, Current Opinion in Colloid & Interface Science. 15 (2010) 73-83.

[28] S. Lu, C. Blanco, S. Appleyard, C. Hammond, B. Rand, Texture studies of carbon and graphite tapes by XRD texture goniometry, Journal of Materials Science. 37 (24) (2002) 5283-5290.

[29] C. Knieke, A. Berger, M. Voigt, R.N. Klupp Taylor, J. Rohrl, W. Peukert, Scalable production of graphene sheets by mechanical delamination, Carbon. 48 (2010) 3196-3204.

[30] C. Teng, D. Xie, J.F. Wang, Z. Yang, G.Y. Ren, Y. Zhu, Ultrahigh conductive graphene paper based on ball-milling exfoliated graphene, Adv. Funct. Mater. 27 (20) (2017) 1700240.

[31] Z.H. Ni, Y.Y. Wang, T. Yu, and Z.X. Shen, Raman spectroscopy and imaging of graphene, Nano Res. 1 (2008) 273-291.

[32] Alexander A. Green, Mark C. Hersam, Solution phase production of graphene with controlled thickness via density differentiation, Nano Lett. 9 (12) (2009) 4031-4036.
[33] Jannik C. Meyer, A. K. Geim, M. I. Katsnelson, K. S. Novoselov, T. J. Booth, S. Roth, The structure of suspended graphene sheets, Nature. 446 (2007) 60-63.
[34] T. Huppertz, Chemistry of the CNs, Advanced Dairy Chemistry. 1A (2013) 135-160.
[35] C. Chen, Z. Xu, Y. Han, H.Y. Sun, C. Gao, Redissolution of flower shaped graphene oxide powder with high density, ACS Appl. Mater. Interfaces. 8 (12) (2016) 8000-8007.
[36] C.F. Ma, X.B. Bi, T. Ngai, G.Z. Zhang, Polyurethane-based nanoparticles as stabilizers for oil-in-water or water-in-oil Pickering emulsions, J. Mater. Chem. A. 1 (17) (2013) 5353-5360.
[37] J.T. Tang, P.J. Quinlan, K.C. Tam, Stimuli-responsive Pickering emulsions: recent advances and potential applications, Soft Matter. 11 (18) (2015) 3512-3529.
[38] X.Y. Zhang, L. Wang, Q. Lu, DL. Kaplan, Mass production of biocompatible graphene using silk nanofibers, ACS Appl. Mater. Interfaces. 10 (27) (2018) 22924-22931.
[39] J.I. Paredes, S. Villar-Rodil, Biomolecule-assisted exfoliation and dispersion of graphene and other two-dimensional materials: a review of recent progress and applications, Nanoscale. 8 (34) (2016) 15389-15413.
[40] Y. Zhang, X.H. Zheng, H.T. Wang, Q.G. Du, Encapsulated phase change materials stabilized by modified graphene oxide, J. Mater. Chem. A. 2 (15) (2014) 5304-5314.
[41] T.D. Dao, H.M. Jeong, A Pickering emulsion route to a stearic acid/graphene core-shell composite phase change material, Carbon. 99 (2016) 49-57.
[42] Q.H Zhao, W.B. Yang, H.P. Zhang, F.F. He, H.J. Yan, R. He, et al., Graphene oxide Pickering phase change material emulsions with high thermal conductivity and photo-thermal performance for thermal energy management, Colloids and Surfaces A. 575 (2019) 42-49.
[43] T. Do, Y.G. Ko, Y.S. Chun, U.S. Choi, Encapsulation of phase change material with water-absorbable shell for thermal energy storage, ACS Sustainable Chem. Eng. 3 (11) (2015) 2874-2881.
[44] T.D. Dao, H.M. Jeong, Novel stearic acid/graphene core-shell composite microcapsule as a phase change material exhibiting high shape stability and performance, Sol. Energy Mater. Sol. Cells. 137 (2015) 227-234.

Declaration of interests

☒ The authors declare that they have no known competing financial interests or personal relationships that could have appeared to influence the work reported in this paper.

☐The authors declare the following financial interests/personal relationships which may be considered as potential competing interests: